



# Kinetic effect of thermal force on impurity transport: Simulation of JT-60SA divertor with integrated divertor code SONIC

K. Shimizu \*, T. Takizuka, H. Kawashima

Japan Atomic Energy Agency, 801-1 Mukoyama, Naka-shi, Ibaraki-ken, 311-0193, Japan

## ARTICLE INFO

PACS:  
52.25.Vy  
52.40.Hf  
52.55.Fa  
52.65.Pp

## ABSTRACT

Using an impurity Monte-Carlo code, IMPMC, the kinetic effect of thermal force on the He transport is investigated for JT-60SA detached plasmas. Without the recycling process, the kinetic effect of the thermal force is found to increase the He density in the divertor region by a factor of  $\sim 2$ , compared with the conventional (fluid) evaluation. However, the kinetic effect is masked by the recycling at the target plates.

© 2009 Elsevier B.V. All rights reserved.

## 1. Introduction

To investigate the plasma and impurity transport in peripheral plasmas, 2D multi-fluid divertor codes have been developed, e.g. B2 [1], EDGE2D [2], UEDGE [3], where impurities are treated as fluid species. The fluid modelling for the impurity transport contains somewhat improper descriptions: (1) assumption of the instantaneous thermalization of impurity ions, (2) neglecting the kinetic effect on the thermal force and (3) simplification for the complicated dissociation processes of hydrocarbons. The Monte-Carlo (MC) approach is suitable for such effects to be taken into account [4]. However, it has the disadvantage for (1) long computational time, (2) large MC noise, and (3) assumption of steady state. Thus, time-evolutional simulations with an MC impurity code coupled self-consistently to a plasma fluid code have not been tried, except for the DORIS impurity code [5]. However, the code coupling between B2-EIRENE and DORIS was limited to the concept and the simulations were carried out for a fixed background plasma [5]. We solved the first and the second problems of the MC modelling by developing a new diffusion model for scattering process and optimizing on the massively parallel computer [6]. Thereby we have developed a coupling of IMPMC [7] code into a 2D divertor code (SOLDOR/NEUT2D) [8]. This integrated code is called SONIC [6]. Recently, we solved the last problem by extending the IMPMC to a time-dependent simulation code, where increasing number of test particles with time is suppressed by a particle reduction scheme [9]. At last, we have obtained a prospect of the coupling of non-steady IMPMC code into the SONIC code.

To demonstrate validity and availability of the SONIC, simulations of dynamic evolution of the X-point MARFE observed in a

JT-60U discharge with low NB heating power of  $P_{\text{NB}} = 5$  MW were carried out [6]. The simulation was also performed for a JT-60U discharge with high NB heating power of  $P_{\text{NB}} = 14$  MW and a very strong gas puff of  $\Gamma_{\text{puff}} = 150$  Pa m<sup>3</sup>/s. Fig. 1 shows the radiation profiles in the detached plasma phase measured in the experiment [10] and that obtained in the simulation with SONIC. The radiation peaks are located at upstream from the strike point and the region with high radiation power extends from the strike point up to near the X-point along the separatrix. These characteristics correspond to experimental data.

The radiation profile in such detached plasma strongly depends on the impurity dynamics, i.e. the balance between the thermal force and the friction force. Taking advantage of the MC modeling of IMPMC code, the kinetic thermal force is investigated in this paper. The simulations are carried out for JT-60SA [11].

## 2. Kinetic thermal force

The impurity retention in the divertor region is basically determined by the balance between the thermal force (toward hotter region in fluid approximation) and the friction force (toward divertor plates). Using a drift kinetic model, the kinetic thermal force was derived by Reiser et al. [12]. In contrast with the fluid thermal force which is averaged over a Maxwellian velocity distribution of impurity ions, the kinetic thermal force was found to have the opposite direction (towards colder region) for impurity ions with high speeds. We independently derived an expression of the kinetic thermal force. The ion thermal force is defined by

$$\vec{R}_{\nabla T_i} = \int m_i \mathbf{v} C(f_i, \delta f_i) d\mathbf{v} \quad (1)$$

where  $C$  is the Fokker–Planck collision operator,  $f_i$  is the distribution function of impurity ions,  $\delta f_i$  is the ion distribution function

\* Corresponding author.

E-mail address: [shimizu.katsuhiko@jaea.go.jp](mailto:shimizu.katsuhiko@jaea.go.jp) (K. Shimizu).

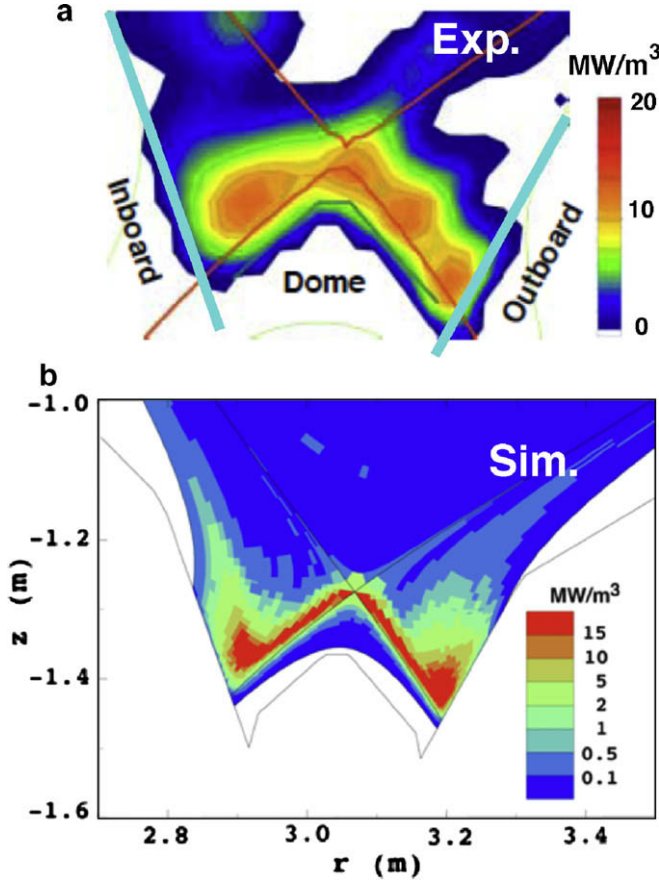


Fig. 1. 2D radiation profile in JT-60U discharge ( $I_p = 1.4$  MA,  $B_T = 3.6$  T,  $P_{NB} = 14$  MW,  $\Gamma_{\text{puff}} = 150$  Pa m<sup>3</sup>/s): (a) experimental data, (b) simulation result with SOLDOR/NEUT2D/IMPIC.

distorted by the ion temperature gradient  $\nabla T_i$ . Substituting  $f_i(\mathbf{v}) = \delta(\mathbf{v} - \mathbf{V}_0)$  into Eq. (1), we obtain the force along the magnetic field line acting on an impurity ion with a velocity  $\mathbf{V}_0$ ,

$$F_{\nabla T_i}(\mathbf{V}_0) \equiv \int d\mathbf{v}' \delta f_i(\mathbf{v}') m_i \{ \Delta \mathbf{v}' \}_i \\ = \int d\mathbf{v}' \delta f_i(\mathbf{v}') \left\{ -\frac{4\pi\lambda e^4 Z_i^2 Z_i^2 \mathbf{u} \cdot \mathbf{b}}{m_{ii} u^3} \right\} \quad (2)$$

where  $m_{ii}$  is the reduced mass,  $\mathbf{u} = \mathbf{V}_0 - \mathbf{v}'$ ,  $\mathbf{b}$  the unit vector along the magnetic field line. Braginskii derived the distorted distribution function by use of Laguerre polynomials [13].

$$\delta f_i(\mathbf{v}) = \frac{n_i}{\pi^{3/2} v_{th}^3} \exp\left(-\frac{m_i}{2T_i} v^2\right) \cdot \tau_i \sum_{n=1}^N a_n L_n^{(3/2)}\left(\frac{m_i}{2T_i} v^2\right) \\ \cdot (\mathbf{v} \cdot \nabla_{\parallel} \ln T_i) \quad (3)$$

where coefficients  $a_n$  are  $a_1 = \frac{26895}{17056}$ ,  $a_2 = \frac{1525}{3198}$ ,  $a_3 = \frac{35}{533}$ . For comparison with Reiser's analytical expression, Eq. (2) is reduced to a non-dimensional form.

$$F_{\nabla T_i}(\mathbf{V}_0) = \left(1 + \frac{m_i}{m_i}\right) \frac{Z_i^2}{Z_i^2} \frac{\partial T_i}{\partial s} \cdot \beta(\mathbf{V}_0, \alpha) \quad (4)$$

$$\beta(\mathbf{V}_0, \alpha) = \frac{3}{\sqrt{2\pi}} \int_0^{\infty} \delta \tilde{f}(x) x^2 I_0(x) dx \quad (5)$$

$$I_0(x) = \int_0^{\pi} -(v_0 \cos \alpha - x \cos \theta) \cos \theta \sin \theta \frac{4E(k^2)}{(a-b)\sqrt{a+b}} d\theta \quad (6)$$

$$\delta \tilde{f}(x) = \sum_{n=1}^3 a_n L_n^{(3/2)}(x^2) \cdot x \exp(-x^2) \quad (7)$$

where  $\alpha$  is an angle between  $\mathbf{V}_0$  and  $\mathbf{b}$ ,  $a = v_0^2 + x^2 - 2v_0x \cos \alpha \cos \theta$ ,  $b = 2v_0x \sin \alpha \sin \theta$ ,  $v_0 = V_0/v_{th}$ ,  $v_{th} = \left(\frac{2T_i}{m_i}\right)^{1/2}$  and  $E(k^2)$  is the complete elliptic integral of the second kind with  $k^2 = \frac{2b}{a+b}$ . The integrations of Eqs. (5) and (6) are carried out numerically by using the Gauss–Legendre integral method. Fig. 2 shows the kinetic thermal force acting on a particle with  $\alpha = 30^\circ$ . The kinetic thermal force derived analytically by Reiser et al. is shown by a broken line. Our result agrees well with their theoretical one.

The kinetic effect may influence impurity density profile a little, because the impurity speed is usually much lower than the background thermal speed. The condition possibly changes for the He ion transport in detached divertor region, where He<sup>2+</sup> ions inflow across the separatrix surface into the SOL region with high speeds and subsequently flow into the cold divertor region. In this situation, the normalized He ion speed may become  $V_0/v_{thi} \sim 1$ . We carry out the simulations of He transport in a detached divertor plasma of JT-60SA [14].

### 3. Background plasma parameter of JT-60SA

JT-60SA (JT-60 Super Advanced) has been programmed to contribute and supplement ITER toward to DEMO. In order to achieve the high performance plasma, the device is equipped with high power and long pulse heating (41MW, 100 s). Thus, the divertor design should be optimized to handle such high heat and particle fluxes. For the lower single null divertor configuration, three types of divertor geometry have been investigated with SOLDOR/NEUT2D code [14]. The 'V-shaped corner' divertor configuration of case B in ref. [14] is similar to that proposed for ITER [15]. The V-shaped corner enhances the recycling at the outer strike point and the detachment is attained there.

The plasma parameter is calculated with SOLDOR/NEUT2D code for the divertor configuration with 'V-shaped corner' shown in Fig. 3(a). The heat flux and the particle flux from the core edge ( $\rho/a = 0.95$ ) are specified,  $Q_{\text{total}} = 37$  MW,  $\Gamma_i = 5 \times 10^{21}$  s<sup>-1</sup>. We assume  $D_{\perp} = 0.25$  m<sup>2</sup>/s for the anomalous particle diffusion coefficient and  $\chi_{\perp}^e = \chi_{\perp}^i = 1$  m<sup>2</sup>/s for the anomalous thermal diffusivity. The recycling coefficient at the divertor plates and walls is set to 1.0 for both ions and neutral particles. The absorption coefficient for neutral particles at the cryopanel is specified so that the

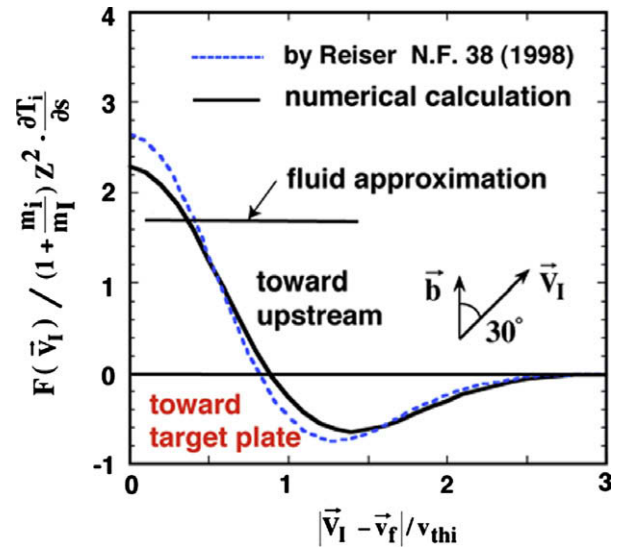
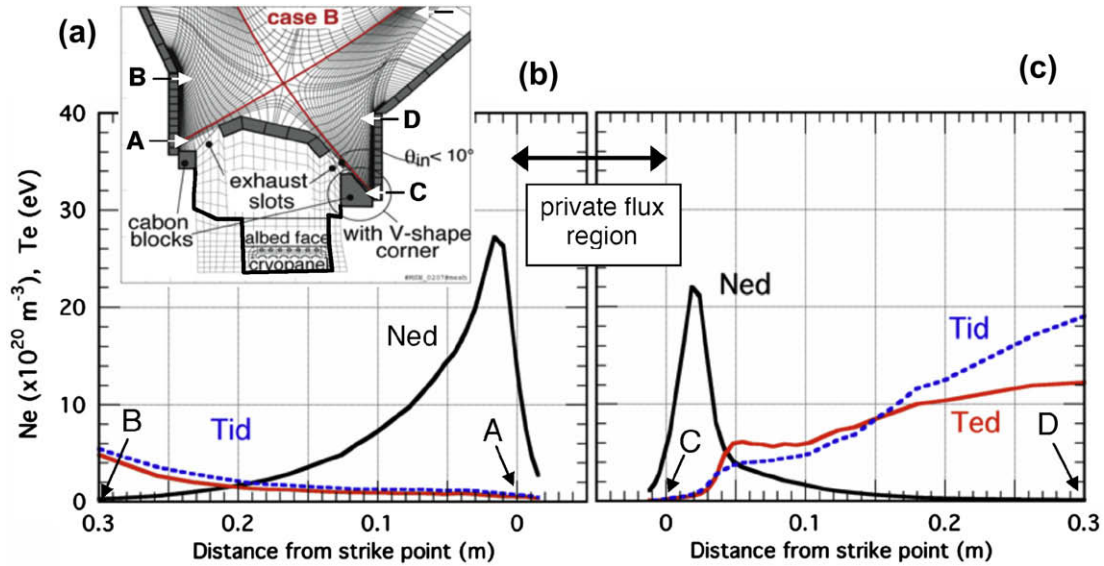


Fig. 2. Kinetic thermal force. It strongly depends on impurity ion speed.



**Fig. 3.** (a) Divertor configuration of JT-60SA with 'V-shaped Corner' and mesh used in the simulations with the SOLDOR/NEUT2D code. Calculated profiles of electron density and temperature in front of (b) the inner target plate and (c) the outer target plate. Both the outer and inner strike points are in the detached state. The points denoted by A, B, C and D correspond to those in (a).

pumping speed is  $S_{\text{pump}} = 50 \text{ m}^3/\text{s}$ . The radiation power of carbon impurities is calculated by a simplified non-corona model, assuming the uniform contamination of  $n_c/n_i = 1\%$  and the residence parameter of  $n_e \tau_{\text{res}} = 4 \times 10^{15} \text{ s/m}^3$ . Without the gas puff, the outer strike point is in the attached state. The gas puff of  $\Gamma_{\text{puff}} = 5 \times 10^{21} \text{ s}^{-1}$  is required to obtain the outer detachment. Fig. 3(b) and (c) show the simulation results; the electron density and temperature at the inner and outer divertor targets.

#### 4. Simulation of He transport with IMPMC

In the impurity Monte-Carlo code (IMPMC), the kinetic equations with the Coulomb collision operator for the distribution func-

tions  $f_i(\mathbf{r}, \mathbf{v}, t)$  are solved using the orbit following Monte-Carlo technique. The model includes (1) impurity generation, (2) ionization of sputtered neutrals, (3) parallel motion of impurity ions along field lines, (4) Coulomb scattering, (5) cross-field diffusion, and (6) atomic processes [6,7].

The kinetic effect of thermal force acting on He ions is investigated with IMPMC code under the detached plasmas of JT-60SA, as shown in Fig. 3. The  $\text{He}^{2+}$  ions are assumed to inflow across the core edge ( $\rho/a = 0.95$ ) uniformly. The  $\text{He}^{2+}$  flux is assumed to be small and not to influence the background plasma. Each test particle has a velocity chosen from the Maxwellian distribution with the plasma ion temperature at the core edge. The He ions which penetrate the interior region ( $\rho/a < 0.95$ ) are simply reflected. In the

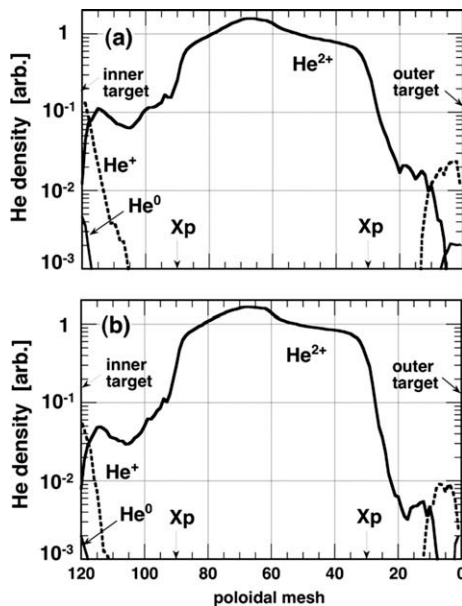


**Fig. 4.** He density profiles along the flux tube close to the separatrix surface, which are calculated neglecting recycling process at the target plates. The kinetic and fluid thermal forces are used in case (a) and case (b), respectively. The kinetic effect enhances the He density near the strike point.

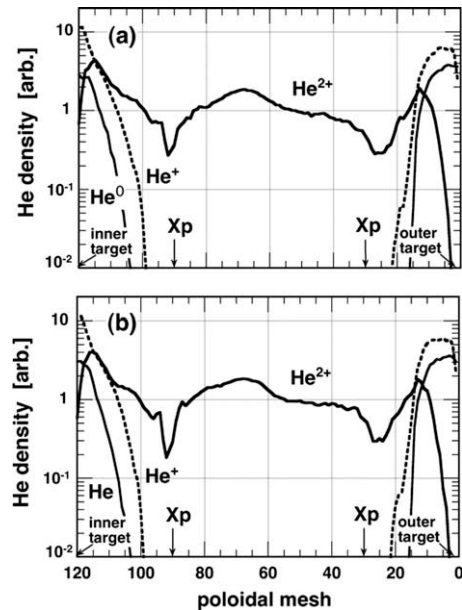


**Fig. 5.** He density profiles along the flux tube close to the separatrix surface, which are calculated including recycling process at the target plates. The kinetic and fluid thermal forces are used in case (a) and case (b), respectively. The kinetic effect on the He density is diminished by the recycling process.

present simulations, ionization and recombination processes are included, but the elastic scattering and charge exchange processes are not included for simplicity.

Firstly, we investigate the effect of the kinetic thermal force on the He compression, excluding the recycling at the divertor plate and the walls. Fig. 4 shows the He density profile in a flux tube close to the separatrix surface. The kinetic effect of the thermal force is found to increase the He density in the divertor region by a factor of  $\sim 2$ , compared with the conventional (fluid) evaluation. The recombination processes become dominant at the front of the divertor plate due to high density and low electron temperature ( $n_{\text{ed}} > 2 \times 10^{21} \text{ m}^{-3}$ ,  $T_{\text{ed}} < 1 \text{ eV}$ ) and the  $\text{He}^{2+}$  density decreases abruptly there.

Secondly, we investigate the total effect including the recycling at the divertor plate and the walls. In the recycling model, a He neutral is emitted with an energy determined from the particle and energy reflection coefficients [16]. The thermalization process of He ion which is ionized after recycling is simulated by Monte-Carlo method, in contrast to the fluid modelling with the assumption of instantaneous thermalization of impurity ions. The kinetic effect is masked by the recycling at the target plates, as shown in Fig. 5. Because the friction force is incomparably larger than the thermal force in the detached region. A small difference, however, exists near the X-point. This difference might change the recycling radially at the divertor plate, depending on the temperature profile along the magnetic field line. In such case, the kinetic thermal force could have a perceptible effect on the He density. Furthermore, the elastic scattering of He neutral with proton collision affects the He transport [17]. The code improvement to incorporate the elastic scattering model is in progress.

## 5. Summary

A self-consistent modelling of divertor plasma and impurity transport has been developed. The feature of this integrated divertor code, SONIC, is to incorporate the elaborate impurity Monte-Carlo code, IMPMC. We overcome the disadvantage of MC modeling, i.e. limitation of time step for Coulomb scattering process,

large MC noise, and assumption of steady state. Currently, the efforts to couple the non-steady IMPMC code to the SONIC code are being made. Taking advantage of the MC modeling in impurity transport, the kinetic thermal force is investigated. Simulations are carried out for the V-shaped corner divertor configuration of JT-60SA. Without the recycling process, the kinetic effect of the thermal force is found to increase the He density in the divertor region by a factor of  $\sim 2$ , compared with the conventional (fluid) evaluation. The kinetic effect is masked by the recycling at the target plates. Model development to include the elastic collision and further study are needed to evaluate the He exhaust, which is one of serious issues for ITER.

## Acknowledgements

They are indebted to Drs T. Ozeki and M. Kikuchi for their continuous encouragement. This work is partly supported by the Grant-in-Aid for Scientific Research on Priority Areas of MEXT (19055005) and by the Grant-in-Aid for Scientific Research (B) of JSPS (18360448).

## References

- [1] R. Schneider et al., *J. Nucl. Mater.* 196–198 (1992) 810.
- [2] R. Simonini et al., *J. Nucl. Mater.* 196–198 (1992) 369.
- [3] T.D. Rognlien et al., *J. Nucl. Mater.* 196–198 (1992) 347.
- [4] K. Shimizu et al., *J. Nucl. Mater.* 241–243 (1997) 167.
- [5] D. Reiser et al., *J. Nucl. Mater.* 290–293 (2001) 953.
- [6] K. Shimizu et al., *J. Nucl. Mater.* 363–365 (2007) 426.
- [7] K. Shimizu et al., *J. Nucl. Mater.* 220–222 (1995) 410.
- [8] K. Shimizu et al., *J. Nucl. Mater.* 313–316 (2003) 1227.
- [9] K. Shimizu et al., *Contribution Plasma Phys.* 48 (1–3) (2008) 270.
- [10] S. Konoshima et al., *J. Nucl. Mater.* 313–316 (2003) 888.
- [11] M. Kikuchi, JA-EU satellite tokamak working group and JT-60SA design team, in: *Proceedings of 21st IAEA Fusion Energy Conference, Chengdu, China, 2006*, IAEA-CN-149/FT/2-5.
- [12] D. Reiser et al., *Nucl. Fus.* 38 (1998) 165.
- [13] S.I. Braginskii et al., *Soviet Phys. JETP* 6 (1958) 358.
- [14] H. Kawashima et al., *Fus. Eng. Des.* 83 (2008) 1643.
- [15] A.S. Kukushkin et al., *Nucl. Fus.* 42 (2002) 187.
- [16] D.N. Ruzic, D.R. Juliano, *J. Nucl. Mater.* 196–198 (1992) 194.
- [17] H. Kubo et al., *Plasma Phys. Control. Fus.* (1999) 747.